International Journal of Architectural, Civil and Construction Sciences
ISSN: 2415-1734
Vol:11, No:9, 2017

Efficiency of Geocell Reinforcement for Using in Expanded Polystyrene Embankments via Numerical Analysis

S. N. Moghaddas Tafreshi, S. M. Amin Ghotbi

Abstract**—**This paper presents a numerical study for investigating the effectiveness of geocell reinforcement in reducing pressure and settlement over EPS geofoam blocks in road embankments. A 3-D FEM model of soil and geofoam was created in ABAQUS, and geocell was also modeled realistically using membrane elements. The accuracy of the model was tested by comparing its results with previous works. Sensitivity analyses showed that reinforcing the soil cover with geocell has a significant influence on the reduction of imposed stresses over geofoam and consequently decreasing its deformation.

Keywords**—**EPS geofoam, road embankments, geocell, reinforcement, lightweight fill.

I. Introduction

USING expanded polystyrene (EPS) geofoam as a geotechnical material has a 50-year-old background in engineering. EPS weighs about 1% of soil and less than 10% of other lightweight fill substitutes. The significant benefit of using such material is the reduction of the imposed loads to the nearby structures or the underlying soil. It is not a common practice to use EPS geofoam for geotechnical applications, but an engineer can tackle certain challenges by its application. It is very easy to handle without using heavy machines, which generally yields in higher construction speed. It is also easier to work with EPS, as it is much less affected by weather conditions and can be shaped and cut anytime on the project site. Finally, it is available in several densities and engineering properties, and retains its initial characteristics through the service life. Its durability is also similar to other construction material [1].

II. Background and Scope of Study

One of the most challenging concerns regarding the use of EPS as filling material for embankments is to find the most effective and reliable pavement system for distributing stress over geofoam and controlling its settlement. For this purpose, a few guidelines have been published on the applications of geofoam in highway embankments among which, NCHRP Web Document 65 and NCHRP report 529, both published in 2004, are two of the most complete ones [2], [3]. However, there are several points of interest for deeper examination which were also explicitly introduced by the above-mentioned materials. “Slope stability issues”, “seismic behavior”, and “effectiveness of using geocell or geogrid above geofoam blocks” are the examples of such topics. The first two topics had the chance to gain more attention by researchers, and several papers and reports have been published about them. However, the use of geogrid or geotextile has attracted much less attention so that there is nearly no direct research on them from 2004 up to now. It is obvious that reinforcement methods (if used consciously) introduce substantial benefits relative to common techniques (e.g. using a concrete slab).

Since the previously cited guidelines contain a conclusive and comprehensive discussion involving main research materials published prior to their publication, we eliminate the repetition of them here. Yet, we just give a short review on a research accomplished in 2000 for its general similarity to our present and future studies.

Reference [4] investigated the behavior of EPS geofoam used as subgrade and fill material under flexible pavement. They performed their tests in a special apparatus simulating the wheel loading more realistically by moving the wheel along an oval-shaped test track. In their test setup, pavement sections included a wearing course, a gravel base layer, and a sand subbase, all of which were positioned over the EPS blocks inside a test box. They examined several effective factors including repeated traffic load, EPS block size, and side restraints. They concluded that resilient deformation of EPS geofoam at the subgrade level is much higher than that for compacted sand. The resilient deformation manifests as a deeper rut on the pavement surface of the EPS geofoam subgrade test section than on the compacted sand subgrade test section, even when both have the same pavement structure. The rut depth could be reduced, however, by using an appropriately designed pavement structure (e.g. increase the pavement thickness or use stiffer pavement).

Reference [5] presented construction and long-term monitoring results for some of embankments with EPS in the I-15 reconstruction project in Salt Lake City. They also used a finite difference program to analyze stress distributions, displacements and strains in specific embankments containing EPS geofoam. Typical configuration of the studied embankments consisted of a 0.6-m base course covered with 0.36-m concrete pavement and no kind of soil reinforcement were investigated.

S. N. Moghaddas Tafreshi is Professor of Geotechnical Engineering, K.N. Toosi University of Technology, Tehran, Iran, 15875-4416 (phone: +98-21-88779474; e-mail: nas_moghaddas@kntu.ac.ir).

S. M. Amin Ghotbi is PhD Candidate, K. N. Toosi University of Technology, Tehran, Iran, 15875-4416 (phone: +98-9124430873; e-mail: aminghotbi@gmail.com).

It is clear from the literature review that there is no direct research on the described topic of using reinforcement of soil above geofoam as a substitute for other methods. A detailed study is beneficent to our knowledge about it and will be valuable for achieving an optimum design procedure. In this study, we aim to utilize a robust numerical method to assess the incorporation of geocell reinforcement with the soil cover over EPS fill to reduce deformation over geofoam blocks and increase pavement's reliability.

III. Numerical Model

Different numerical methods are available for analyzing stress-strain in engineering applications. Finite Element Method (FEM) is one of the most popular, easy, and accurate methods for this purpose. This method is available in many commercial and non-commercial software packages such as ABAQUS, ANSYS, PLAXIS, etc. ABAQUS has great capabilities including robust mesh generation techniques, loading patterns, and constitutive laws for using in geotechnical applications. ABAQUS was considered to be a proper choice for our studies according to the mentioned points.

In this study, material properties and model dimensions were selected based on our future experimental program and laboratory settings. Soil properties and reinforcement have a meaningful relation with those in the research of [6]. Thus, we compare our results with it and further references to ensure its correctness.

A. Geometry, Loading and Boundary Conditions

The future physical model will consist of a 2×2.5 m box in plan and 90 cm in height. The walls and bottom of the box are constructed from rough and rigid concrete. Loads will be applied to the soil through a circular rigid steel plate with the diameter of 30 cm, which represents a typical tire loading area according to [6]. Soil and geofoam will be placed in the box according to test plans. In the numerical model, sides were fixed in the horizontal direction and set free in the vertical direction. It was observed that the boundary fixity in the horizontal direction will not impose any certain inaccuracies to the results. The dimensions of the box are sufficient to remove any interference with the soil stresses from plate loading. Geocell will be placed at a specific depth in order to prevent damage from direct contact with the rigid plate during loading. A typical geometry of the model and the geocell created in ABAQUS are shown in Fig. 1.

B. Material Models and Properties

Material properties were kept in close consistency with those of [7] in order to derive comparable results for validation of the model. A linear Drucker-Prager model available in ABAQUS was used to simulate plastic deformations in the soil and geofoam. This model is capable of reproducing stress distribution more accurately compared to traditional Mohr-Coulomb model. Soil's Young's modulus and Poisson's ratio were set to 30 MPa and 0.4, respectively. Its angle of friction and dilation angle was also selected 45° and 15°, respectively. For geocell, a simple elastic model with Young's modulus of 200 MPa and Poisson's ratio of 0.35 was derived from [8]. For EPS, Mohr-Coulomb model values were chosen from [9]. Table I shows the values of different parameters for soil, geocell, and EPS.

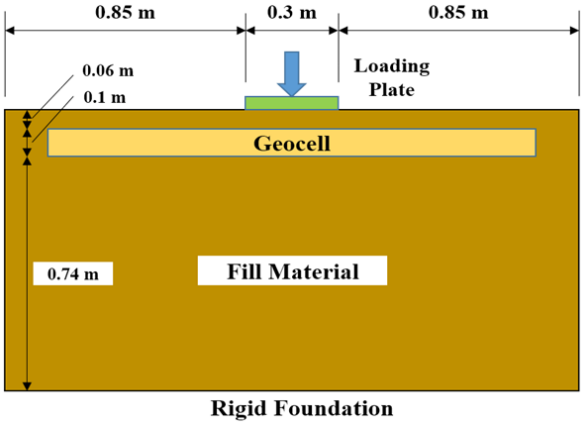

(a)

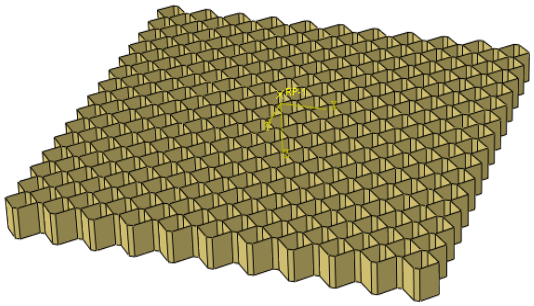

(b)

Fig. 1 (a) Geometry of the embankment system. (b) Geometry of geocell in ABAQUS

TABLE I
Material Properties

	Material	Soil	EPS 30	Geocell
Basic Properties	Density (kg/m^3)	2000	30	333
	Young's Modulus (MPa)	30	7.8	200
	Poisson's Ratio	0.4	0.17	0.35
Plastic Properties	Angle of Friction	45	2	-
	Cohesion (kPa)	-	62	-
	Dilation Angle	15	0.1	-
	Yield Stress (kPa)	18	-	-
	Flow Stress Ratio	0.78	-	-

C. FE Mesh Details

As large deformations were expected for achieving the final bearing pressure during the analysis, a full scale 3D model was created and meshed as shown in Fig. 2. For the validation part (which does not include EPS blocks), a total number of 71744 hexahedral linear elements with reduced integration formulation (C3D8R) were used for soil. Elements around the plate edge were sized around 4 mm to enable calculating extensive deformation and stress gradient in the soil under

extreme loadings. It is also worth mentioning that finer mesh was also used for the soil near the ground surface. It is clear that element's size was increased wherever higher accuracies were not needed.

Geocell was modeled with a total number of 14830 with linear membrane elements (M3D4R). An embedded interaction was used between soil and geocell and it yielded very good results for our study. This interaction assumes that soil and geocell fully move together and it saves computational cost to a great extent while generating reliable results.

D. Analysis Procedure

Geostatic stresses were established through soil medium via a primary step applying soil body forces. On the next step, the foundation pressure was applied to a circular rigid plate atop the soil. The loading was increase until large deformations occurred. The interaction between the rigid plate and soil was considered to be "Frictionless" for tangential behavior and "Hard Contact" for the normal one. Loads for the both steps were applied through a smooth loading pattern to assure reduction of numerical errors originated from dynamic effects accompanied with more suddenly applied patterns (e.g. linear pattern).

Explicit solver was selected for analyzing the system and obtaining the final results. The explicit method uses very small time increments and could produce accurate results if used properly. It was observed that the results obtained from explicit method had a very little difference with the implicit or static ones, while providing a much faster analysis.

E. Validation

According to Fig. 3 vertical pressure in soil at depth of 300 mm increase with the applied pressure for both unreinforced and geocell reinforced cases, and their values are very close to each other until the applied pressure reaches to about 600 kPa. This result is compatible with those obtained by [7] when the underlying and cover material has the same stiffness. In fact, the stiffness of the reinforcing material has to be considerably larger than the values used in this research in order to mobilize the mattressing effect when both material has the same stiffness. However, for larger deformations where a substantial part of the soil under the foundation has reached its plastic limit, the geocell exhibits the effectiveness in reducing the vertical stress at this depth. For both reinforced and unreinforced graphs, the value of the stresses locates under the dashed line indicating the amount of applied pressure. When the soil is unreinforced, its pressure at the 30-cm depth draws back to the applied pressure after a certain pressure reaches a certain value (600 kPa for this case), due to the loss in soil strength after yielding.

Fig. 4 demonstrates the variations of bearing pressure with the footing settlement. Pressure was applied on the foundation until it reached an ultimate state. According to this figure, geocell reinforcement increases the bearing pressure of the foundation by at least 50% although there is no significant difference in footing settlement for the pressures less than 400 kPa.

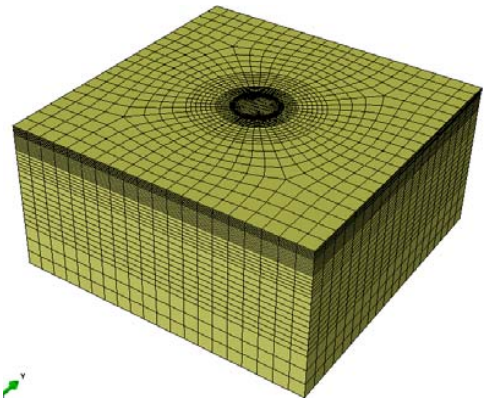

Fig. 2 FEM Mesh

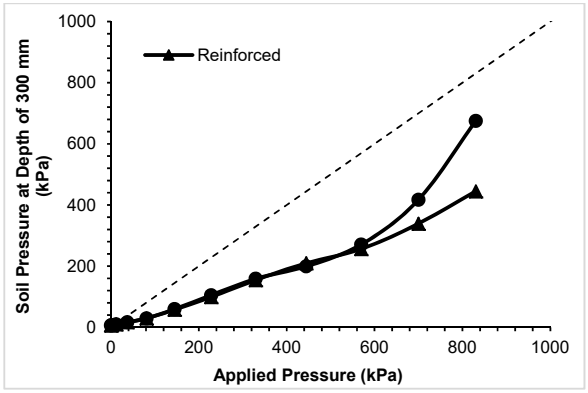

Fig. 3 Variation of transferred pressure with applied pressure on the footing surface

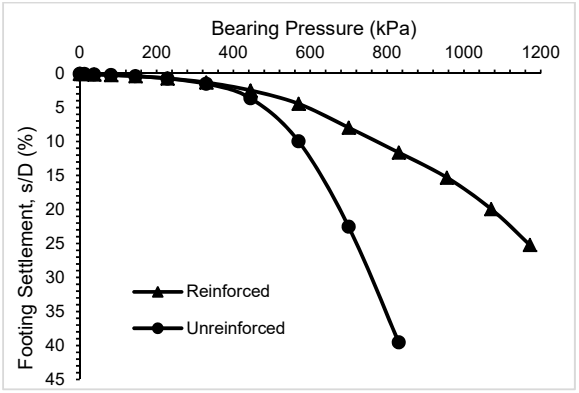

Fig. 4 Variation of bearing pressure with footing settlement

IV. Results

In this section, the influence of EPS density is discussed for a model section with a soil cover of thickness 30 cm. The detailed properties of various EPS densities are given in Table II.

Bearing pressure of the footing versus its settlement for different densities of EPS is illustrated in Fig. 5. The density

of each EPS type is indicated by their value in the legend, and the reinforcement status is specified with the letters "R" for reinforced and "U" for unreinforced in front of it. The words "Top" and "Bottom" in the figures refer to top of geofoam fill and under geofoam fill, respectively. It is concluded that the bearing pressure of all cases are less than that of the basic model (with no geofoam) except the reinforced case of EPS 30. In fact, the combined use of EPS 30 with geocell has caused a slight growth in the bearing pressure of the foundation. Consequently, EPS 30 was selected as the suitable density for the use in road embankments. It should be noted that the authors did not have access to the mechanical properties of higher densities of EPS at this time. It is therefore obvious that if higher densities show significant improvement in the performance and cost effectiveness simultaneously, their usage would be justifiable over lower densities.

TABLE II
EPS PROPERTIES

Material Properties	EPS 15	EPS 20	EPS 30
Density (kg/m^3)	15	20	30
Young's Modulus (MPa)	2.4	4	7.8
Poisson's Ratio	0.1	0.12	0.17
Friction Angle	1.5	2	2.5
Cohesion (kPa)	33.75	38.75	62

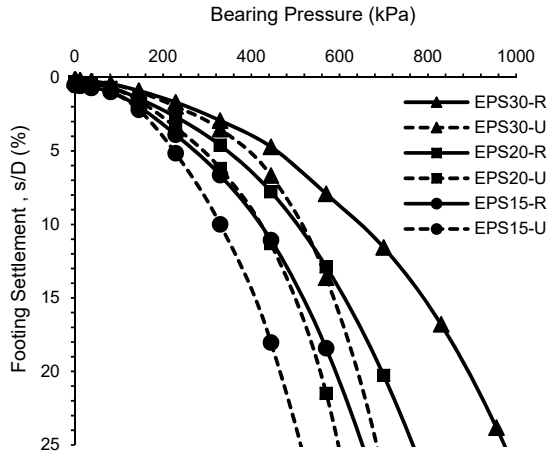

Fig. 5 Variation of bearing pressure with footing settlement for different EPS densities

Fig. 6 displays top and bottom pressure distribution profiles of EPS15 for both reinforced and unreinforced cases. All pressures were measured when the foundation pressure reached 700 kPa. In agreement with the observations for the case study in the validation part, geocell reinforcement exhibits a great capability in reduction of stresses over very soft fill material like EPS15. The vertical pressure over and under geofoam had reductions of about 30% and 44% respectively for the reinforced case compared to unreinforced case. When the reinforcement is present, the stress distribution diagram has been flattened, and a more uniform stress profile was obtained. The reason is that geocell spreads the load over a wider area by its special reinforcing mechanisms. Such behavior is beneficent when using EPS in road embankments, as it is critical to avoid concentrated stress on the geofoam.

Figs. 7 and 8 display the pressure distribution on the top and bottom of geofoam in unreinforced and reinforced states for EPS20 and EPS30, respectively. While the amount of vertical pressure on the top and bottom of geofoam increases with increase in geofoam density, the percent of reduction between the reinforced and unreinforced cases decreases. For example, the pressure on top of EPS block reduces from 213 kPa to 163 kPa for EPS20 (24% reduction) and from 249 kPa to 205 kPa for EPS 30 (18% reduction). Comparing percentage of variation in the pressure over geofoams with different densities, increasing the density and Young's modulus of EPS results in a higher increase of pressure over geofoam for reinforced cases.

Although increasing geofoam densities leads to the reduction of pressure in the bottom of EPS blocks (over the foundation) in the unreinforced cases, it causes an increase for the reinforced ones. Comparing the effect of reinforcement for each density, there are considerable decrease in the pressure under geofoam in the reinforced cases relative to unreinforced ones for EPS15 and EPS20. For EPS30, there is a slight increase in the vertical stress under geofoam for the reinforced case compared to unreinforced case which can be assumed unimportant.

To summarize, geocell reinforcement generally has a significant influence on the reduction of vertical stresses applied over EPS blocks. The amount of reduction varies from 30% for EPS15 to 18% for EPS30. For the bottom of geofoam, this reduction is 42% and 27% for EPS15 and EPS30 and 14% increase for EPS30.

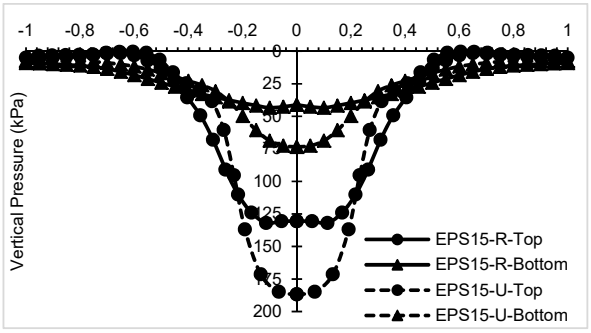

Fig. 6 Pressure distribution over and under geofoam for reinforced and unreinforced cases at 700 kPa

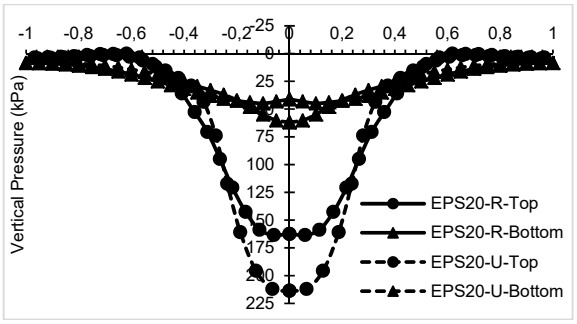

Fig. 7 Pressure distribution over and under geofoam for reinforced and unreinforced cases at 700 kPa

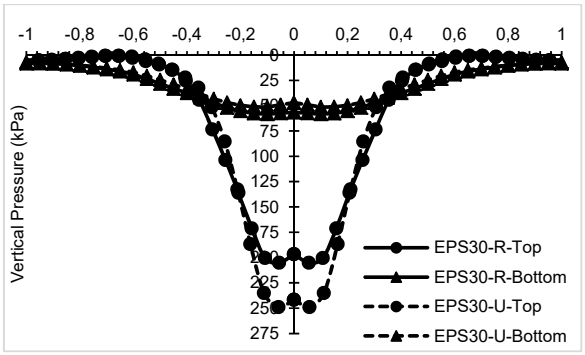

Fig. 8 Pressure distribution over and under geofoam for reinforced and unreinforced cases at 700 kPa

REFERENCES

[1] Stark, T. D., Bartlett, S. F., Arellano, D., "Expanded Polystyrene (EPS) Geofoam Applications and Technical Data," The EPS Industry Alliance, 2012.

[2] Stark, T. D., Arellano, D., Horvath, J. S., and Leshchinsky, D., "NCHRP Web Document 65 (Project 24-11): Geofoam Applications in the Design and Construction of Highway Embankments," Transportation Research Board, Washington, D.C., 2004.

[3] Stark, T. D., Arellano, D., Horvath, J. S., and Leshchinsky, D., "NCHRP Report 529: Guideline and Recommended Standard for Geofoam Applications in Highway Embankments," Transportation Research Board, Washington, D.C., 2004.

[4] Zou, Y., Small, J. C. and Leo, C. J., "Behavior of EPS Geofoam as Flexible Pavement Subgrade Material in Model Tests," Geosynthetics International, vol. 7, no. 1, pp. 1-22, 2000.

[5] Newman, M. P., Bartlett, S. F. and Lawton, E. C., "Numerical Modeling of Geofoam Embankments," J. Geotech. Geoenviron. Eng., vol. 136, pp. 290-298, 2010.

[6] Brito, L. A. T., Dawson, A. R. and Kolisoja, P. J., "Analytical Evaluation of Unbound Granular Layers in Regard to Permanent Deformation," in Bearing Capacity of Roads, Railways and Airfields. 8th International Conference, 2009.

[7] Leshchinsky, B. and Ling, H. I., "Numerical modeling of behavior of railway ballasted structure with geocell confinement," Geotextiles and Geomembranes, vol. 36, pp. 33-43, 2013.

[8] Moghaddas Tafreshi, S. N., Khalaj, O. and Dawson, A. R., "Pilot-scale load tests of a combined multilayered geocell and rubber-reinforced foundation," Geosynthetics International, vol. 20, no. 3, pp. 143-161, 2013.

[9] Lal B. R. R., Padade, A. H. and Mandal, J. N., "Numerical Simulation of EPS Geofoam as Compressible Inclusions in Fly Ash Backfill Retaining Walls," in Geo-Shanghai 2014, Shanghai, China, 2014.